

# Direct Observation of C–O Reductive Elimination from Palladium Aryl Alkoxide Complexes To Form Aryl Ethers

Ross A. Widenhoefer, H. Annita Zhong, and Stephen L. Buchwald\*

Contribution from the Department of Chemistry, Massachusetts Institute of Technology, Cambridge, Massachusetts 02139

Received September 23, 1996<sup>⊗</sup>

**Abstract:** Reaction of KOCH<sub>2</sub>CMe<sub>3</sub> with [(*R*)-Tol-BINAP]Pd(*p*-C<sub>6</sub>H<sub>4</sub>CN)Br formed [(*R*)-Tol-BINAP]Pd(*p*-C<sub>6</sub>H<sub>4</sub>CN)(OCH<sub>2</sub>CMe<sub>3</sub>) (**5**) in quantitative yield (<sup>1</sup>H NMR spectroscopy). Thermolysis of **5** in THF-*d*<sub>8</sub> at 47 °C led to C–O reductive elimination with formation of *p*-neopentoxybenzotrile (85 ± 2%). A secondary P–C bond-cleavage process led to formation of 4,4'-dimethylbiphenyl (16 ± 2%). Kinetic analysis of the decomposition of **5** at 47 °C in the presence of excess potassium neopentoxide established the two-term rate law, rate = *k*[**5**] + *k'*[**5**][KOCH<sub>2</sub>CMe<sub>3</sub>], where *k* = 1.50 ± 0.07 × 10<sup>-3</sup> s<sup>-1</sup> and *k'* = 6.2 ± 0.4 × 10<sup>-3</sup> s<sup>-1</sup> M<sup>-1</sup>, consistent with reductive elimination via competing alkoxide-dependent and alkoxide-independent pathways. In addition, excess KOCH<sub>2</sub>CMe<sub>3</sub> exchanged rapidly with the palladium-bound alkoxide ligand of **5** at 47 °C according to the rate law: rate exchange = *k*<sub>ex</sub>[**5**][KOCH<sub>2</sub>CMe<sub>3</sub>], where *k*<sub>ex</sub> = 1.0 ± 0.1 × 10<sup>2</sup> s<sup>-1</sup> M<sup>-1</sup>. Thermolysis of the related palladium *p*-cyanophenyl alkoxide complexes (P–P)Pd(*p*-C<sub>6</sub>H<sub>4</sub>CN)(OR) [P–P = (*S*)-BINAP, R = CH<sub>2</sub>CMe<sub>3</sub>; P–P = (*R*)-Tol-BINAP, R = CHMe<sub>2</sub>, CMe<sub>3</sub>; P–P = dppf, R = CH<sub>2</sub>CMe<sub>3</sub>, CMe<sub>3</sub>] and (dppf)Pd[*o*-C<sub>6</sub>H<sub>4</sub>(CH<sub>2</sub>)<sub>2</sub>C(Me)<sub>2</sub>O] led to aryl ether formation in 46–91% yield.

## Introduction

Reductive elimination from a low-valent group 10 metal center to form an (aryl)C–C bond represents the key bond-forming step in a variety of synthetically relevant catalytic cross-coupling protocols.<sup>1</sup> As a result, the mechanisms of C–C reductive elimination from well-defined group 10 metal complexes have been intensely investigated.<sup>2</sup> Similarly, C–N and C–S reductive elimination presumably serve as the key bond-forming steps in the corresponding palladium-catalyzed cross-coupling protocols,<sup>3,4</sup> and reductive elimination from well-characterized group 10 metal aryl amido<sup>5</sup> and aryl sulfido<sup>6</sup> complexes to form arylamines and aryl sulfides, respectively,

<sup>⊗</sup> Abstract published in *Advance ACS Abstracts*, July 1, 1997.

(1) (a) Stille, J. K. *Angew. Chem., Int. Ed. Engl.* **1986**, *25*, 508. (b) Miyaura, N.; Suzuki, A. *Chem. Rev.* **1995**, *95*, 2457. (c) de Meijere, A.; Meyer, F. E. *Angew. Chem., Int. Ed. Engl.* **1994**, *33*, 2379.

(2) (a) Collman, J. P.; Hegedus, L. S.; Norton, J. R.; Finke, R. G. In *Principles and Applications of Organotransition Metal Chemistry*; University Science: Mill Valley, CA, 1987; p 322. (b) Stille, J. K. In *The Chemistry of the Metal–Carbon Bond, Vol. II. The Nature and Cleavage of the Metal–Carbon Bond*; Hartley, F. R., Patai, S., Eds.; Wiley: New York, 1985; pp 625–787.

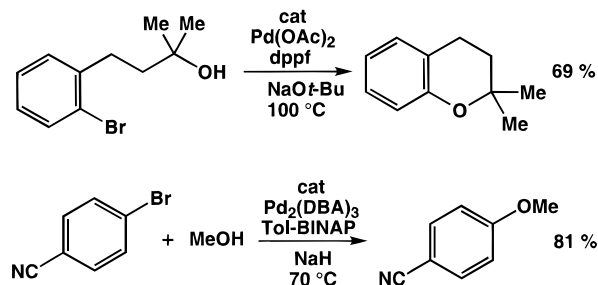
(3) (a) Kosugi, M.; Ogata, T.; Terada, M.; Sano, H.; Migita, T. *Bull. Chem. Soc. Jpn.* **1985**, *58*, 3657. (b) Takagi, K. *Chem. Lett.* **1987**, 2221. (c) Dickens, M. J.; Gilday, J. P.; Mowlem T. J.; Widdowson, D. A. *Tetrahedron* **1991**, *47*, 8621. (d) Carpita, A.; Rossi, R.; Scamuzzi, B.; *Tetrahedron Lett.* **1989**, *30*, 2699. (e) Cristau, H. J.; Chabaud, B.; Chene, A.; Christol, H. *Synthesis* **1981**, 892.

(4) (a) Kosugi, M.; Kameyama, M.; Migita, T. *Chem. Lett.* **1983**, 927. (b) Guram, A. S.; Buchwald, S. L. *J. Am. Chem. Soc.* **1994**, *116*, 7901. (c) Guram, A. S.; Rennels, R. A.; Buchwald, S. L. *Angew. Chem., Int. Ed. Engl.* **1995**, *34*, 1348. (d) Wolfe, J. P.; Buchwald, S. L. *J. Org. Chem.* **1996**, *61*, 1133. (e) Wolfe, J. P.; Rennels, R. A.; Buchwald, S. L. *Tetrahedron* **1996**, *52*, 7525. (f) Wolfe, J. P.; Wagaw, S.; Buchwald, S. L. *J. Am. Chem. Soc.* **1996**, *118*, 7215. (g) Driver, M. S.; Hartwig, J. F. *J. Am. Chem. Soc.* **1996**, *118*, 7217. (h) Wagaw, S.; Buchwald, S. L. *J. Org. Chem.* **1996**, *61*, 7240. (i) Paul, F.; Patt, J.; Hartwig, J. F. *J. Am. Chem. Soc.* **1994**, *116*, 5969. (j) Louie, J.; Hartwig, J. F. *Tetrahedron Lett.* **1995**, *36*, 3609.

(5) (a) Driver, M. S.; Hartwig, J. F. *J. Am. Chem. Soc.* **1996**, *118*, 4206. (b) Villanueva, L. A.; Abboud, K. A.; Boncella, J. M. *Organometallics* **1994**, *13*, 3921. (c) Koo, K.; Hillhouse, G. L. *Organometallics* **1995**, *14*, 4421. (d) Koo, K.; Hillhouse, G. L. *Organometallics* **1996**, *15*, 2669. (e) Berryhill, S. R.; Price, T.; Rosenblum, M. *J. Org. Chem.* **1983**, *48*, 158.

(6) Bärnanno, D.; Hartwig, J. F. *J. Am. Chem. Soc.* **1995**, *117*, 2937.

## Scheme 1



has been observed. However, despite numerous examples of group 10 metal aryl alkoxide complexes, direct thermal reductive elimination to form an (aryl)C–O bond has not been observed.<sup>7,8</sup>

We have recently developed a palladium-catalyzed procedure for the formation of aryl ethers from aryl bromides and alcohols that employed bulky bidentate phosphine ligands such as 1,1'-bis(diphenylphosphino)ferrocene (dppf), 2,2'-bis(di-*p*-tolylphosphino)-1,1'-binaphthyl [Tol-BINAP], or 2,2'-bis(diphenylphosphino)-1,1'-binaphthyl [BINAP] in the presence of a base (Scheme 1). For example, treatment of (2-bromophenyl)-2-methyl-2-butanol with a catalytic amount of Pd(OAc)<sub>2</sub> and dppf and a stoichiometric quantity of sodium *tert*-butoxide led to ring closure and formation of 2,2-dimethylchroman in 69% yield (Scheme 1).<sup>9</sup> Likewise, cross-coupling of 4-bromobenzonitrile and methanol in the presence of excess sodium hydride was efficiently catalyzed by a mixture of Pd<sub>2</sub>(DBA)<sub>3</sub> and Tol-BINAP, forming *p*-methoxybenzotrile in 81% yield (Scheme 1).<sup>10</sup> Significantly, these systems appeared to provide an opportunity to observe (aryl)C–O reductive elimination from a group 10 metal center. Here we report the generation of

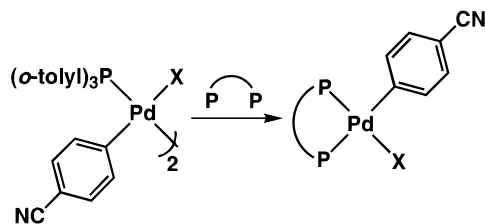
(7) Bryndza, H. E.; Tam, W. *Chem. Rev.* **1988**, *88*, 1163.

(8) After this paper was submitted, an example of aryl(C)–O reductive elimination from a palladium (aryl)*tert*-butoxide complex was reported by Hartwig: Mann, G.; Hartwig, J. F. *J. Am. Chem. Soc.* **1996**, *118*, 13109.

(9) Palucki, M.; Wolfe, J. P.; Buchwald, S. L. *J. Am. Chem. Soc.* **1996**, *118*, 10333.

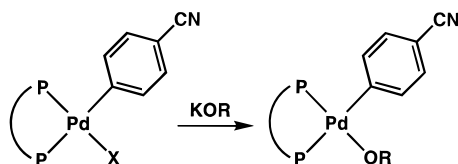
(10) Palucki, M.; Wolfe, J. P.; Buchwald, S. L. *J. Am. Chem. Soc.* **1997**, *119*, 3395.

## Scheme 2



X	P-P	PdX	yield
Br	Tol-BINAP	1	94 %
I	Tol-BINAP	2	75 %
Br	BINAP	3	80 %
Br	dppf	4	79 %

## Scheme 3



P-P	R	PdOR
Tol-BINAP	CH <sub>2</sub> CMe <sub>3</sub>	5
BINAP	CH <sub>2</sub> CMe <sub>3</sub>	6
Tol-BINAP	CHMe <sub>2</sub>	7
Tol-BINAP	CMe <sub>3</sub>	8
Tol-BINAP	<i>p</i> -C <sub>6</sub> H <sub>4</sub> Me	9
dppf	CH <sub>2</sub> CMe <sub>3</sub>	10
dppf	CMe <sub>3</sub>	11

thermally unstable palladium aryl alkoxide complexes that undergo reductive elimination to form aryl ethers.

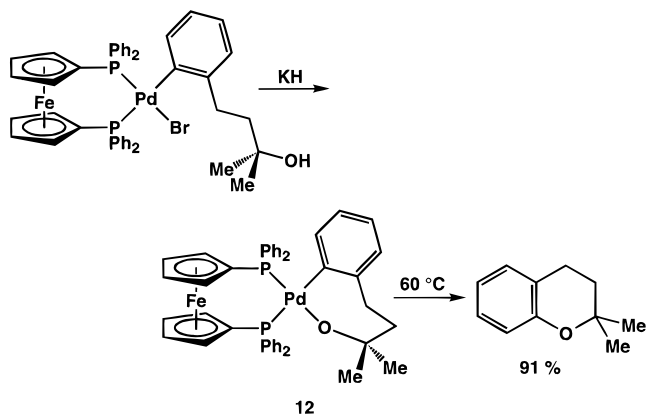
## Results

**Formation of Palladium Aryl Alkoxide Complexes.** Our approach to generate palladium aryl alkoxide complexes with bidentate phosphine ligands involved metathesis of a palladium *p*-cyanophenyl halide complex with potassium neopentoxide. Neopentoxide was initially employed due to its diagnostic signals in the <sup>1</sup>H NMR spectrum and because neopentanol coupled efficiently with 4-bromobenzonitrile under catalytic conditions.<sup>11</sup> The requisite palladium *p*-cyanophenyl halide complexes [(*R*)-Tol-BINAP]Pd(*p*-C<sub>6</sub>H<sub>4</sub>CN)(Br) (**1**), [(*S*)-Tol-BINAP]Pd(*p*-C<sub>6</sub>H<sub>4</sub>CN)(I) (**2**), [(*S*)-BINAP]Pd(*p*-C<sub>6</sub>H<sub>4</sub>CN)(Br) (**3**), and (dppf)Pd(*p*-C<sub>6</sub>H<sub>4</sub>CN)(Br) (**4**) were prepared in good yield (>75%) from reaction of the appropriate combination of ligand and palladium tri-*o*-tolylphosphine dimer  $\{[Pd(P(o-tolyl)_3](p-C_6H_4CN)(\mu-X)]_2$  (X = Br, I) (Scheme 2). Complexes **1–4** were characterized by standard spectroscopic techniques and elemental analysis.

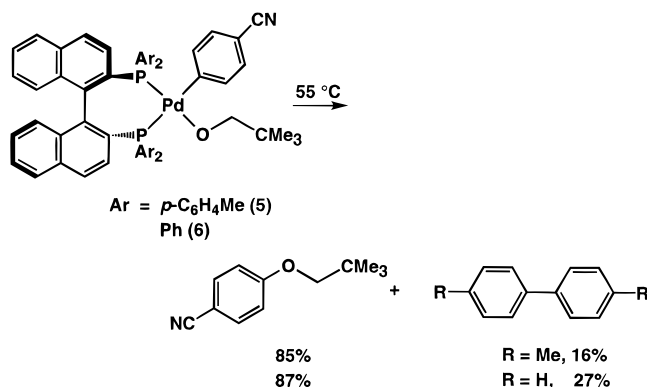
Treatment of a pale yellow solution of **1** in THF-*d*<sub>8</sub> with a slight excess (~1.1 equiv) of potassium neopentoxide rapidly formed an orange solution of the palladium neopentoxide complex [(*R*)-Tol-BINAP]Pd(*p*-C<sub>6</sub>H<sub>4</sub>CN)(OCH<sub>2</sub>CMe<sub>3</sub>) (**5**) in quantitative yield by <sup>1</sup>H NMR spectroscopy (Scheme 3). Likewise, reaction of KOCH<sub>2</sub>CMe<sub>3</sub> with iodide precursor **2** also generated **5** as the exclusive palladium species. Solutions of **5** darkened within minutes at room temperature, and attempts to isolate **5** from the corresponding preparative-scale reaction were unsuccessful. As a result, alkoxide complex **5** was characterized

(11) Palucki, M.; Buchwald, S. L. Unpublished results.

## Scheme 4



## Scheme 5



by <sup>1</sup>H and <sup>31</sup>P NMR spectroscopy without isolation. The <sup>1</sup>H NMR spectrum of **5** in THF-*d*<sub>8</sub> displayed a 1:1:1:1 ratio of *p*-tolyl peaks at  $\delta$  2.38, 2.19, 1.98, and 1.93 and a single *tert*-butyl resonance at  $\delta$  0.17; the ratio of these resonances established the 1:1 ratio of neopentoxide ligands to [Tol-BINAP]-PdAr groups. A pair of doublets at  $\delta$  2.76 and 2.62 ( $J \approx 9$  Hz) assigned to the diastereotopic methylene protons of the alkoxide ligand confirmed binding of the alkoxide to the chiral metal fragment. The <sup>31</sup>P NMR spectrum of **5** displayed two doublets at  $\delta$  29.3 and 14.1 ( $J_{PP} = \sim 37$  Hz), which established bidentate coordination of the phosphine ligand to the palladium alkoxide fragment.<sup>12</sup>

The related palladium *p*-cyanophenyl alkoxide complexes (P-P)Pd(*p*-C<sub>6</sub>H<sub>4</sub>CN)(OR) [P-P = (*S*)-BINAP, R = CH<sub>2</sub>CMe<sub>3</sub> (**6**); P-P = (*R*)-Tol-BINAP, R = CHMe<sub>2</sub> (**7**), CMe<sub>3</sub> (**8**), *p*-C<sub>6</sub>H<sub>4</sub>Me (**9**); P-P = dppf, R = CH<sub>2</sub>CMe<sub>3</sub> (**10**), CMe<sub>3</sub> (**11**)] were formed by analogous procedures. In each case, the desired palladium alkoxide complex was formed as the exclusive palladium species by <sup>1</sup>H and <sup>31</sup>P NMR spectroscopy and was characterized without isolation. In addition, the oxapalladacycle

(dppf)Pd[*o*-C<sub>6</sub>H<sub>4</sub>(CH<sub>2</sub>)<sub>2</sub>C(Me)<sub>2</sub>O] (**12**) was isolated free from KBr and excess alkoxide in 77% yield from treatment of the aryl bromide complex (dppf)Pd[*o*-C<sub>6</sub>H<sub>4</sub>(CH<sub>2</sub>)<sub>2</sub>C(Me)<sub>2</sub>OH]Br with KH in THF at room temperature (Scheme 4). Palladacycle **12** was characterized by spectroscopy and elemental analysis. For example, the <sup>1</sup>H NMR spectrum of **12** displayed a pair of singlets at  $\delta$  0.55 and 0.07 assigned to the diastereotopic methyl resonances, which established alkoxide coordination to palladium.

(12) Formation of a stable five-coordinate anionic palladium complex possessing both an alkoxide ligand and a halide ligand appears highly unlikely. For example, treatment of a 1:1 mixture of **1** and **2** with 1 equiv of KOCH<sub>2</sub>CMe<sub>3</sub> generated a single species (**5**) as determined by <sup>1</sup>H and <sup>31</sup>P NMR spectroscopy at -52 °C.

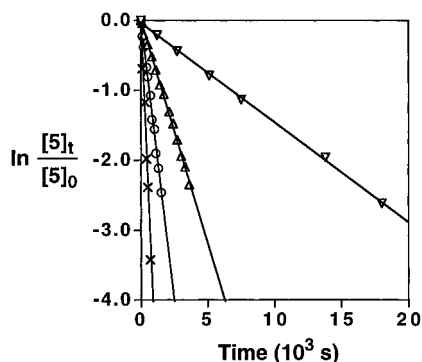


**Figure 1.** Representative first-order plots for disappearance of **5** in THF-*d*<sub>8</sub> at 23 (∇), 37 (Δ), 47 (○), and 55 °C (×).

**Table 1.** First-Order Rate Constants and Aryl Ether Yield for Thermal Decomposition of Complexes **5–12** ([Pd]<sub>0</sub> ≈ 1.5 × 10<sup>-2</sup> M) in THF-*d*<sub>8</sub>

compd	<i>T</i> (°C)	[KOR] (mM)	10 <sup>4</sup> <i>k</i> <sub>obs</sub> (s <sup>-1</sup> )	ArOR (%)
5	23	<2	1.43 ± 0.01	76
5	23	<2	1.45 ± 0.02 <sup>a</sup>	72
5	35	<2	5.2 ± 0.2	
5	37	<2	6.3 ± 0.2	
5	47	<2	15.3 ± 0.4	85
5	47	<2	15.6 ± 0.2 <sup>b</sup>	71
5	47	<2	16.7 ± 0.3 <sup>c</sup>	75
5	47	<2	16.1 ± 0.3 <sup>d</sup>	72
5	47	43	18.1 ± 0.6	97
5	47	110	20.9 ± 0.6	97
5	47	120	23.0 ± 0.9	
5	47	170	23.2 ± 0.3	94
5	47	200	25.5 ± 0.9	
5	47	260	33 ± 1	
5	47	280	33 ± 1	
5	52	<2	30 ± 1	
5	55	<2	43 ± 2	85
5	55	<2	45 ± 3 <sup>a</sup>	87
5	57	<2	58 ± 2	86
6	47	<2	15.1 ± 0.2	87
7	23	<2		66
8	55	<2	14.1 ± 0.7	61
9	60	<2	0.13 ± 0.01	<5
10	55	<2	14.3 ± 0.6	46
11	55	<2	10.3 ± 0.6	47
12	60	<2	11.1 ± 0.6	91

<sup>a</sup> Contained PPh<sub>3</sub> (0.15 M). <sup>b</sup> Contained KOTf (98 μmol/mL). <sup>c</sup> Contained KOTf (180 μmol/mL). <sup>d</sup> Contained excess KBr (270 μmol/mL).

### Thermolysis of Palladium Aryl Alkoxide Complexes.

Neopentoxide complex **5** decomposed rapidly at or above room temperature to form mixtures of aryl ether and biaryl side products (Scheme 5). For example, thermolysis of a freshly prepared solution of **5** in THF-*d*<sub>8</sub> at 47 °C led to first-order decay to >3 half-lives with an observed rate constant of *k*<sub>obs</sub> = 1.53 × 10<sup>-3</sup> s<sup>-1</sup> (*t*<sub>1/2</sub> = 7.5 min) (Figure 1, Table 1).<sup>13</sup> <sup>1</sup>H NMR and GCMS analysis of the resulting black solution revealed the formation of *p*-neopentoxybenzotrile (85 ± 2%) and 4,4'-dimethylbiphenyl (16 ± 2%). No significant amounts (<3%) of products resulting from β-hydrogen elimination,<sup>14</sup> P/Pd aryl

(13) (a) Rate measurements employing different batches of **5** and KOCH<sub>2</sub>CMe<sub>3</sub> provided values for *k*<sub>obs</sub> that differed by <7.5%. (b) These solutions contained small amounts (<2 mM) of free KOCH<sub>2</sub>CMe<sub>3</sub> and 1 equiv of KBr. Despite the small concentration of free alkoxide present under these conditions, the reaction rate is dominated by the first-order pathway *k* >> *k'*[KOCH<sub>2</sub>CMe<sub>3</sub>] and *k*<sub>obs</sub> ≈ *k*; the rate of decomposition of **5** generated with <1 equiv of alkoxide was not significantly different. Thermolysis of **5** in the presence of excess KBr (270 μmol/mL) or thermolysis of **5** generated from iodide precursor **2** led to no significant change in the rate or efficiency of reductive elimination. However, the effect of 1 equiv KBr on C–O reductive elimination from **5** is not known.

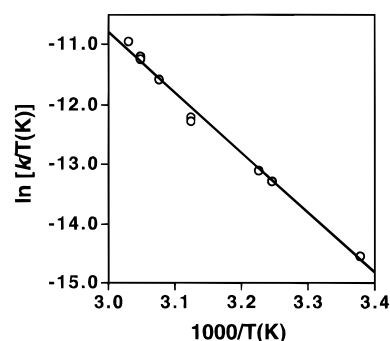


**Figure 2.** Eyring plot for the thermolysis of **5** in THF-*d*<sub>8</sub> over the temperature range 23–57 °C.

exchange,<sup>15</sup> or P–C bond hydrogenolysis were observed. Likewise, no significant resonances corresponding to free or ligated Tol-BINAP were observed by <sup>1</sup>H or <sup>31</sup>P NMR spectroscopy of the final reaction mixture.<sup>16</sup> Observed rate constants for disappearance of **5** were also obtained at temperatures ranging from 23 to 57 °C in THF-*d*<sub>8</sub> (Figure 1, Table 1).<sup>13</sup> An Eyring plot of the data provided the activation parameters: Δ*H*<sup>‡</sup> = 19.8 ± 0.8 kcal mol<sup>-1</sup>; Δ*S*<sup>‡</sup> = -9.3 ± 0.3 eu (Figure 2).

Thermolysis of **5** in the presence of PPh<sub>3</sub> (0.15 M) as a trapping agent led to no significant change in rate of decomposition or yield of *p*-neopentoxybenzotrile (Table 1) but eliminated formation of 4,4'-dimethylbiphenyl. The failure of PPh<sub>3</sub> to enhance the yield of aryl ether formation is in contrast to C–S reductive elimination from related (dppe)Pd(aryl)SCMe<sub>3</sub> complexes [dppe = (diphenylphosphino)ethane], which required the presence of a trapping agent to generate high yields of thioether.<sup>6</sup> In contrast, thermolysis of **5** in the presence of KOCH<sub>2</sub>CMe<sub>3</sub> increased both the rate of decomposition and the yield of *p*-neopentoxybenzotrile (Table 1). In order to determine the rate dependence on neopentoxide concentration, observed rate constants for decomposition of **5** were measured as a function of KOCH<sub>2</sub>CMe<sub>3</sub> concentration from 0.0017 to 0.30 M at 47 °C in THF-*d*<sub>8</sub> (Table 1). A plot of *k*<sub>obs</sub> versus alkoxide concentration was linear with a significant positive intercept of the ordinate, which established the two-term rate law shown in eq 1, where *k* = 1.50 ± 0.07 × 10<sup>-3</sup> s<sup>-1</sup> (Δ*G*<sup>‡</sup> = 22.9 ± 0.1 kcal mol<sup>-1</sup>) and *k'* = 6.2 ± 0.4 × 10<sup>-3</sup> s<sup>-1</sup> M<sup>-1</sup> (Δ*G*<sup>‡</sup> = 22.0 ± 0.1 kcal mol<sup>-1</sup>) (Figure 3). It is noteworthy that the rate of decomposition of **5** in THF-*d*<sub>8</sub> was not significantly accelerated (≤10%) in the presence of potassium salts such KOTf (98–180 μmol/mL) (Table 1).

$$\text{rate} = -\frac{d[\mathbf{5}]}{dt} = k[\mathbf{5}] + k'[\mathbf{5}][\text{KOCH}_2\text{CMe}_3] \quad (1)$$

In addition to promoting reductive elimination, excess KOCH<sub>2</sub>CMe<sub>3</sub> underwent rapid, associative exchange with the

(14) (a) Bryndza, H. E.; Calabrese, J. C.; Marsi, M.; Roe, D. C.; Tam, W.; Bercaw, J. E. *J. Am. Chem. Soc.* **1986**, *108*, 4805. (b) Goldman, A. S.; Halpern, J. *J. Am. Chem. Soc.* **1987**, *109*, 7537. (c) Hoffman, D. M.; Lappas, D.; Wierda, D. A. *J. Am. Chem. Soc.* **1993**, *115*, 10538. (d) Blum, O.; Mielstein, D. *Angew. Chem., Int. Ed. Engl.* **1995**, *34*, 229. (e) Bernard, K. A.; Rees, W. M.; Atwood, J. D. *Organometallics* **1986**, *5*, 390.

(15) (a) Morita, D. K.; Stille, J. K.; Norton, J. R. *J. Am. Chem. Soc.* **1995**, *117*, 8576. (b) Kong, K.-C.; Cheng, C.-H. *J. Am. Chem. Soc.* **1991**, *113*, 6313. (c) Segelstein, B. E.; Butler, T. W.; Chenard, B. L. *J. Org. Chem.* **1995**, *60*, 12. (d) Gillie, A.; Stille, J. K. *J. Am. Chem. Soc.* **1980**, *102*, 4933.

(16) The <sup>1</sup>H NMR spectrum of the reaction mixture revealed a broad resonance at δ 2.1 possibly corresponding to (*R*)-Tol-BINAP palladium complexes, while the <sup>31</sup>P NMR spectrum displayed a broad resonance at δ ~2. No resonances in the region expected for free (*R*)-Tol-BINAP (δ -16.1) or Pd[*R*]-Tol-BINAP]<sub>2</sub> were observed. The <sup>31</sup>P NMR resonance for Pd-[*R*]-BINAP]<sub>2</sub> is δ ~25 [Ozawa, F.; Kubo, A.; Hayashi, T. *Chem. Lett.* **1992**, 2177].

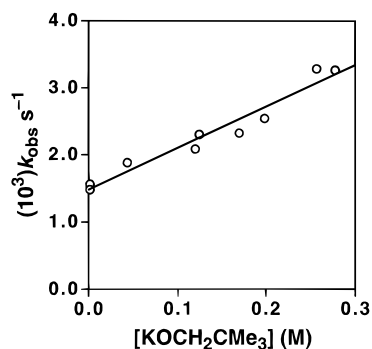


**Figure 3.** Potassium neopentoxide concentration dependence of the rate of reductive elimination of **5** in THF-*d*<sub>8</sub> at 47 °C.

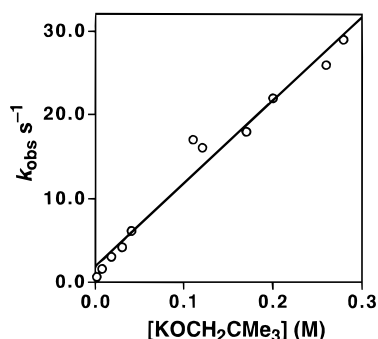


**Figure 4.** Potassium neopentoxide concentration dependence of the rate of alkoxide exchange with **5** in THF-*d*<sub>8</sub> at 47 °C.

palladium-bound neopentoxide group of **5**. For example, in the <sup>1</sup>H NMR spectrum of **5** at 55 °C, the resonances for the neopentoxide ligand remained sharp with no loss of coupling between the diastereotopic methylene protons. However, addition of KOCH<sub>2</sub>CMe<sub>3</sub> led to considerable broadening of these resonances in the <sup>1</sup>H NMR spectrum. Observed rate constants for alkoxide exchange were determined from excess <sup>1</sup>H NMR line broadening ( $\Delta\omega_{1/2} = k/\pi$ )<sup>17</sup> of the *tert*-butyl resonance of **5** as a function of alkoxide concentration from 0.0017 to 0.3 M KOCH<sub>2</sub>CMe<sub>3</sub> at 47 °C. A plot of *k*<sub>obs</sub> versus [KOCH<sub>2</sub>CMe<sub>3</sub>] established the first-order dependence of the rate of exchange on alkoxide concentration and the second-order rate law shown in eq 2, where  $k_{\text{ex}} = 1.0 \pm 0.1 \times 10^2 \text{ s}^{-1} \text{ M}^{-1}$  ( $\Delta G^\ddagger = 15.8 \pm 0.1 \text{ kcal mol}^{-1}$ ) at 47 °C (Figure 4). The second-order rate constant for alkoxide exchange (*k*<sub>ex</sub>) is >5 orders of magnitude greater than the second-order rate constant for reductive elimination (*k*').

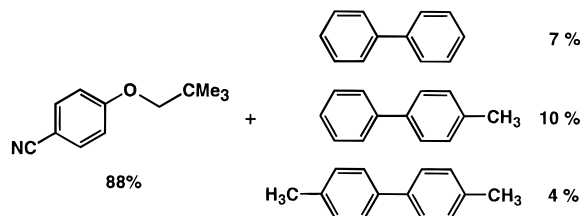
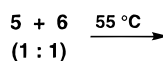
$$\text{rate of alkoxide exchange} = k_{\text{ex}}[\mathbf{5}][\text{KOCH}_2\text{CMe}_3] \quad (2)$$

Thermolysis of BINAP-ligated complex **6** at 47 °C in THF-*d*<sub>8</sub> also led to first-order decomposition at a rate not significantly different from that of **5**, with formation of *p*-neopentoxybenzotrile (87 ± 2%) and biphenyl (27 ± 2%) (Table 1, Scheme 5). The formation of biphenyl from **6** and 4,4'-dimethylbiphenyl from **5** strongly implicates the phosphorus-bound aryl groups as the source of biaryl side products.<sup>18</sup> The presence of a phosphine degradation pathway is also consistent with the absence of significant resonances corresponding to either free or bound phosphine ligand in the <sup>1</sup>H or <sup>31</sup>P NMR of the final

(17) Bovey, F. A. *Nuclear Magnetic Resonance Spectroscopy*, 2nd ed.; Academic Press: San Diego, CA, 1988.

(18) (a) Garrou, P. E. *Chem. Rev.* **1985**, *85*, 171. (b) Coulson, D. R. *Chem. Commun.* **1968**, 1530. (c) Fahey, D. R.; Mahan, J. E. *J. Am. Chem. Soc.* **1976**, *98*, 4499. (d) Taylor, N. J.; Chieh, P. C.; Carty, A. J. *J. Chem. Soc., Chem. Commun.* **1975**, 448. (e) Blake, D. M.; Nyman, C. J. *J. Am. Chem. Soc.* **1970**, *92*, 5359. (f) Bellon, P. L.; Ceriotti, A.; Demartin, F.; Longoni, G.; Heaton, B. T. *J. Chem. Soc., Dalton Trans.* **1982**, 1671.

### Scheme 6



reaction mixtures generated by thermolysis of **5** or **6**. Although the ultimate fate of palladium in these thermolysis reactions is unclear, thermal decomposition of group 10 transition metal phosphine complexes has been shown to generate  $\mu$ -phosphide clusters.<sup>18</sup>

In an effort to distinguish between intra- and intermolecular pathways for the formation of biaryl side products in the decomposition of complexes **5** and **6**, an equimolar mixture of **5** and **6** was thermolyzed and analyzed for cross-over products (Scheme 6).<sup>19</sup> Intramolecular biaryl formation should form biphenyl and 4,4'-dimethylbiphenyl only, while an intermolecular process is expected to form a statistical 1.0:2.6:1.7 mixture of 4,4'-dimethylbiphenyl, 4-phenyltoluene, and biphenyl. Significantly, thermolysis of a 1.0 ± 0.1:1 mixture of **5** and **6** at 55 °C produced a 1.0:2.5:1.8 mixture of 4,4'-dimethylbiphenyl, 4-phenyltoluene, and biphenyl in 21% total yield, consistent with biaryl formation via an intermolecular process.

Thermal decomposition of isopropoxide complex **7** was considerably faster than decomposition of **5**. Although kinetics were not performed, the half-life for decomposition of **7** at 23 °C was ≤5 min, which is ≥15 times faster than decomposition of **5** under comparable conditions. Analysis of the resulting solution revealed formation of *p*-isopropoxybenzotrile (66%), benzotrile (22%), and 4,4'-dimethylbiphenyl (18%) (Scheme 7, Table 1). The yield of *p*-isopropoxybenzotrile formed in the thermolysis of **7** increased to 81% in the presence of excess KOCHMe<sub>2</sub>. Reductive elimination from the *tert*-butoxide complex **8** in THF-*d*<sub>8</sub> at 55 °C was approximately three times slower than reductive elimination from neopentoxide complex **5** with formation of *p-tert*-butoxybenzotrile (61%) and 4,4'-dimethylbiphenyl (26%) (Scheme 7, Table 1). Thermal decomposition of the *p*-cresolate complex **9** was >450 times slower than decomposition of neopentoxide complex **5** and led to no detectable formation of diaryl ether.

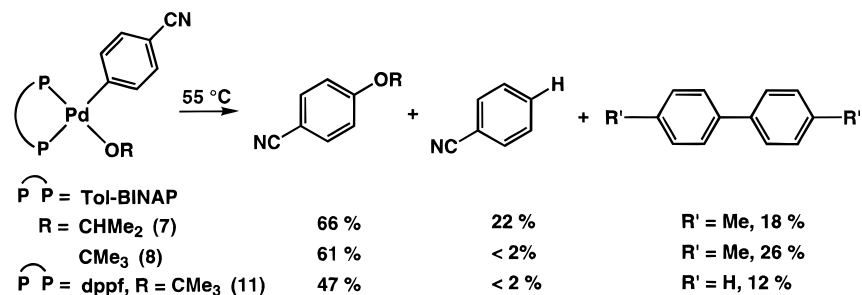
Thermal decomposition of the dpfp-ligated palladium aryl alkoxide complexes was also investigated. For example, thermal decomposition of **10** at 55 °C in THF-*d*<sub>8</sub> led to first-order decay at a rate approximately three times slower than decomposition of **5** under comparable conditions (Table 1). Analysis of the resulting black solution revealed the formation of *p*-neopentoxybenzotrile (46%), pivaldehyde (36%), benzotrile (43%), and biphenyl (12%) (Table 1, Scheme 8). Thermolysis of *tert*-butoxide complex **11** at 55 °C formed *p-tert*-butoxybenzotrile (47%) and biphenyl (12%) (Scheme 7), while thermolysis of tertiary oxapalladacycle complex **12** at 60 °C in THF-*d*<sub>8</sub> produced 2,2-dimethylchroman in high yield (91%) (Scheme 4).

### Discussion

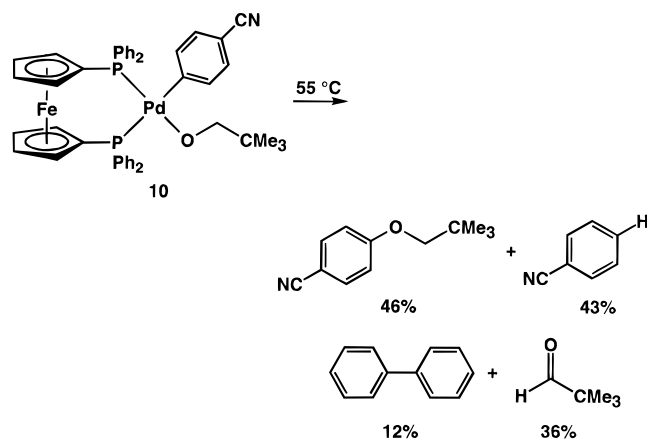
**C–O Bond Formation.** Thermolysis of palladium aryl alkoxide complexes led to C–O reductive elimination and

(19) The *S* enantiomer [(*S*)-Tol-BINAP]Pd(*p*-C<sub>6</sub>H<sub>4</sub>CN)OCH<sub>2</sub>CMe<sub>3</sub> generated from [(*S*)-Tol-BINAP]Pd(*p*-C<sub>6</sub>H<sub>4</sub>CN)Br was employed in these cross-over experiments.

## Scheme 7



## Scheme 8



formation of aryl ethers. Reductive elimination to form an (aryl)C–O bond is unprecedented, and related C–O reductive elimination processes have been observed in only two cases.<sup>8</sup> For example, thermolysis of the palladium bis(phosphine) acyl aryloxy complex  $(\text{PPh}_2)_2\text{Pd}(\text{COMe})(\text{OAr})$  led to C–O reductive elimination and formation of aryl esters.<sup>20</sup> The analogous nickel complexes underwent C–O reductive elimination upon addition of  $\pi$ -acids such as acrylonitrile or CO.<sup>20</sup> Likewise, treatment of the nickel aryloxy complex  $(\text{phen})\text{Ni}(\text{O}-o\text{-C}_6\text{H}_4\text{-CMe}_2\text{CH}_2)$  ( $\text{phen} = 1,10\text{-phenanthralene}$ ) with  $\text{I}_2$  formed 4,4-dimethyl-3,4-dihydrocoumarin in 55% yield.<sup>21</sup> C–O reductive elimination is also implicated in a variety of stoichiometric transformations,<sup>22</sup> as well as nickel-,<sup>23</sup> palladium-,<sup>24</sup> and copper-catalyzed<sup>25</sup> reactions. Several related transformation such as C–O bond cleavage<sup>26</sup> and O–H reductive elimination<sup>27</sup> have also been observed.

The experimental rate law for decomposition of **5** (eq 1) in the presence of  $\text{KOCH}_2\text{CMe}_3$  is consistent with C–O reductive elimination via competing alkoxide-dependent and alkoxide-independent pathways. The first-order rate dependence on

palladium concentration and the activation parameters ( $\Delta H^\ddagger = 19.8 \pm 0.8 \text{ kcal mol}^{-1}$ ;  $\Delta S^\ddagger = -9.3 \pm 0.3 \text{ eu}$ ) for the alkoxide-independent pathway are consistent with unimolecular reductive elimination directly from **5** to form *p*-neopentoxybenzonitrile and  $\text{Pd}[\text{Tol-BINAP}]$ .<sup>13</sup> The latter species is expected to be highly reactive<sup>28</sup> and presumably decomposes via P–C bond cleavage to form 4,4'-dimethylbiphenyl (see below).

We considered two plausible mechanisms for the unimolecular reductive elimination pathway. One pathway is a concerted process analogous to that proposed for H–H, C–H, and C–C reductive elimination (Scheme 9, path a).<sup>2</sup> Although our kinetics do not distinguish this pathway from a mechanism initiated by rapid and reversible dissociation of a single phosphorus center, C–S,<sup>6</sup> C–C,<sup>29,30</sup> and C–H<sup>31</sup> reductive elimination have been shown to occur directly from a four-coordinate platinum group bis(phosphine) complex without prior ligand dissociation. We also considered a mechanism initiated by inner-sphere nucleophilic attack of the alkoxide ligand at the ipso carbon atom of the palladium-bound aryl group via a Meisenheimer-type species such as **I** (Scheme 9, path b).<sup>32</sup> This C–O reductive elimination pathway is analogous to the mechanisms proposed for  $\alpha$ -migrat-

(25) (a) Keegstra, M. A.; Peters, T. H. A.; Brandsma, L. *Tetrahedron* **1992**, *48*, 3633. (b) Aalten, H. L.; van Koten, G.; Grove, D. M.; Kuilman, T.; Piekstra, O. G.; Hulshof, L. A.; Sheldon, R. A. *Tetrahedron* **1989**, *45*, 5565. (c) Capdevielle, P.; Maumy, M. *Tetrahedron Lett.* **1993**, *34*, 1007. (d) Nobel, D. *J. Chem. Soc., Chem. Commun.* **1993**, 419. (e) Pert, D. J.; Ridley, D. D. *J. Chem.* **1989**, *42*, 421. (f) Whitesides, G. M.; Sadowski, J. S.; Lilburn, J. *J. Am. Chem. Soc.* **1974**, *96*, 2829. (g) Lindley, J. *Tetrahedron* **1984**, *40*, 1433. (h) Bacon, R. G. R.; Rennison, S. C. *J. Chem. Soc. C* **1969**, 308. (i) Bacon, R. G. R.; Rennison, S. C. *J. Chem. Soc. C* **1969**, 312.

(26) Yamamoto, A. *Adv. Organomet. Chem.* **1992**, *34*, 111.

(27) Glueck, D. S.; Winslow, L. J. N.; Bergman, R. G. *Organometallics* **1991**, *10*, 1462.

(28) Otsuka, S. *J. Organomet. Chem.* **1980**, *200*, 191.

(29) Stang, P. J.; Kowalski, M. H. *J. Am. Chem. Soc.* **1989**, *111*, 3356.

(30) Braterman, P. S.; Cross, R. J.; Young, G. B. *J. Chem. Soc., Dalton Trans.* **1977**, 1892.

(31) (a) Michelin, R. A.; Faglia, S.; Uguagliati, P. *Inorg. Chem.* **1983**, *22*, 1831. (b) Abis, L.; Sen, A.; Halpern, J. *J. Am. Chem. Soc.* **1978**, *100*, 2915.

(32) A mechanism initiated by intermolecular attack of the Pd–O bond of **5** at the ipso carbon atom of a second molecule of **5** is not in accord with the first-order dependence of the reaction rate on **[5]**. Likewise, a mechanism initiated by rate-limiting alkoxide dissociation is not in line with the experimental entropy of activation. However, we cannot distinguish the pathway shown in Scheme 9, path b, from a mechanism initiated by rapid and reversible alkoxide dissociation to form  $[\text{Tol-BINAP}]\text{Pd}(p\text{-C}_6\text{H}_4\text{-CN})^+$   $[\text{OCH}_2\text{CMe}_3]^-$ , followed by attack of the alkoxide at the ipso carbon atom.

(33) (a) Dockter, D. W.; Fanwick, P. E.; Kubiak, C. P. *J. Am. Chem. Soc.* **1996**, *118*, 4846. (b) Bryndza, H. E.; Calabrese, J. C.; Wreford, S. S. *Organometallics* **1984**, *3*, 1603. (c) Bryndza, H. E.; Kretchmar, S. A.; Tulip, T. H. *J. Chem. Soc., Chem. Commun.* **1985**, 977. (d) Michelin, R. A.; Napoli, M.; Ros, R. *J. Organomet. Chem.* **1979**, *175*, 239. (e) Bennett, M. A.; Yoshida, T. *J. Am. Chem. Soc.* **1978**, *100*, 1750. (f) Arnold, D. P.; Bennett, M. A.; Crisp, G. T.; Jeffery, J. C. *Adv. Chem. Ser.* **1982**, *196*, 195. (g) Bennett, M. A. *J. Organomet. Chem.* **1986**, *300*, 7. (h) Bennett, M. A.; Rokicki, A. *Aust. J. Chem.* **1985**, *38*, 1307. (i) Appleton, T. G.; Bennett, M. A. *J. Organomet. Chem.* **1973**, *55*, C88. (j) Bennett, M. A. *J. Mol. Catal.* **1987**, *41*, 1. (k) Bennett, M. A.; Rokicki, A. *J. Organomet. Chem.* **1983**, *244*, C31. (l) Bennett, M. A.; Rokicki, A. *J. Organometallics* **1985**, *4*, 180. (m) Bryndza, H. E. *Organometallics* **1985**, *4*, 1686.

(20) Komiya, S.; Akai, Y.; Tanaka, K.; Yamamoto, T.; Yamamoto, A. *Organometallics* **1985**, *4*, 1130.

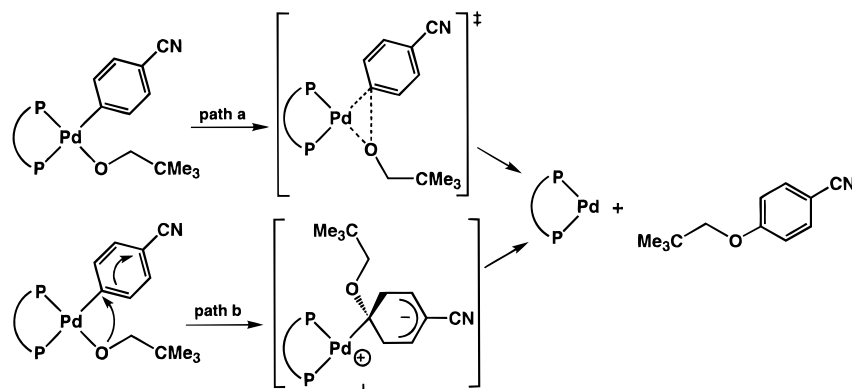
(21) (a) Koo, K.; Hillhouse, G. L.; Rheingold, A. L. *Organometallics* **1995**, *14*, 456. (b) Matsunaga, P. T.; Mavropoulos, J. C.; Hillhouse, G. L. *Polyhedron* **1995**, *14*, 175.

(22) (a) Bernard, K. A.; Churchill, M. R.; Janik, T. S.; Atwood, J. D. *Organometallics* **1990**, *9*, 12. (b) Komiya, S.; Tane-ichi, S.; Yamamoto, A.; Yamamoto, T. *Bull. Chem. Soc. Jpn.* **1980**, *53*, 673. (c) Bryndza, H. E.; Calabrese, J. C.; Wreford, S. S. *Organometallics* **1984**, *3*, 1603.

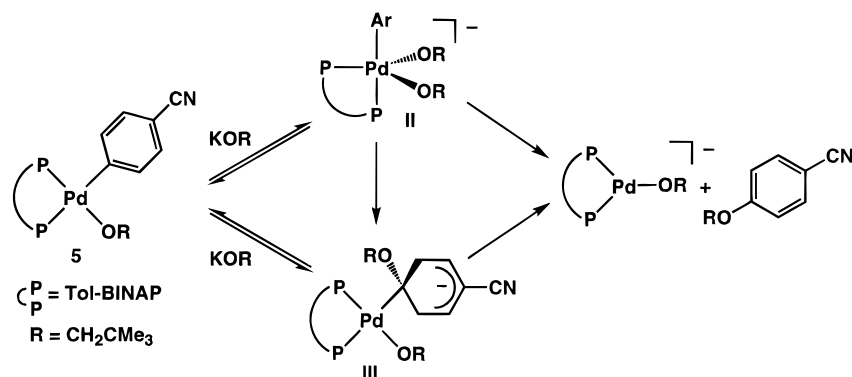
(23) (a) Cristau, H.-J.; Cesmurs, J. *Ind. Chem. Libr.* **1995**, *7*, 240. (b) Cramer, R.; Coulson, D. R. *J. Org. Chem.* **1975**, *40*, 2267.

(24) (a) Kundu, N. G.; Pal, M.; Mahanty, J. S.; Dasgupta, S. K. *J. Chem. Soc., Chem. Commun.* **1992**, 41. (b) Stanton, S. A.; Felman, S. W.; Parkhurst, C. S.; Godleski, S. A. *J. Am. Chem. Soc.* **1983**, *105*, 1964. (c) Larock, R. C.; Gou, L. *Synlett* **1995**, 465. (d) Larock, R. C.; Berrios-Peña, N. G.; Fried, C. A. *J. Org. Chem.* **1991**, *56*, 2615. (e) Larock, R. C.; Berrios-Peña, N. G.; Fried, C. A.; Yum, E. K.; Tu, C.; Leong, W. *J. Org. Chem.* **1993**, *58*, 4509. (f) Larock, R. C.; Harrison, L. W.; Hsu, M. H. *J. Org. Chem.* **1984**, *49*, 3664. (g) Larock, R. C.; Berrios-Peña, N. G.; Narayanan, K.; *J. Org. Chem.* **1990**, *55*, 3447.

## Scheme 9



## Scheme 10



tory insertion of both CO<sup>33</sup> and isocyanides<sup>34</sup> into group 10 metal–alkoxide bonds.<sup>7</sup> The high nucleophilicity of late-transition-metal alkoxide ligands is evidenced by the strong tendency of the oxygen atom of these complexes to serve as a hydrogen-bond acceptor in the presence of free alcohols.<sup>35</sup>

Several experimental observations point to an insertion mechanism (path b) in preference to a symmetric concerted pathway (path a). For example, the decreasing rate of C–O reductive elimination in the order OCHMe<sub>2</sub> (**7**) > OCH<sub>2</sub>CMe<sub>3</sub> (**5**) > OCMe<sub>3</sub> (**8**) ≫ OC<sub>6</sub>H<sub>4</sub>Me (**9**) appears unusual for concerted reductive elimination<sup>36</sup> but roughly parallels the nucleophilicity of the respective palladium hydrocarboxide. In addition, preliminary studies probing the electronic effects indicate that the rate of C–O reductive elimination increases dramatically with the decreasing electron density of the palladium-bound aryl group.<sup>37</sup> The extent of rate acceleration appears greater than

that expected through strictly inductive effects and strongly suggests the delocalization of negative charge within the aryl ligand in the transition state for C–O reductive elimination.

The rate of reductive elimination from **5** was accelerated in the presence of potassium neopentoxide. The absence of significant rate acceleration in the presence of potassium salts such as KOTf argues against a medium effect and points to a mechanism initiated by direct attack of potassium neopentoxide on **5**. One possible mechanism involves rapid and reversible attack of neopentoxide at palladium to generate the anionic five-coordinate bis(alkoxide) intermediate {[Tol-BINAP]Pd(*p*-C<sub>6</sub>H<sub>4</sub>-CN)(OCH<sub>2</sub>CMe<sub>3</sub>)<sub>2</sub>}<sup>−</sup> (**II**) (Scheme 10).<sup>38</sup> Rate-limiting C–O reductive elimination from **II** would then generate *p*-neopentoxybenzonitrile and the three-coordinate palladium alkoxide fragment {[Tol-BINAP]Pd(OCH<sub>2</sub>CMe<sub>3</sub>)<sup>−</sup>}. Alternately, inner-sphere (**II** → **III**) or outer sphere (**5** → **III**) attack of alkoxide at the ipso-carbon atom of the palladium-bound aryl group would form the palladium alkoxide Meisenheimer complex **III** (Scheme 10). Collapse of intermediate **III** via Pd–C bond cleavage would then generate *p*-neopentoxybenzonitrile and {[Tol-BINAP]Pd(OCH<sub>2</sub>CMe<sub>3</sub>)<sup>−</sup>}.<sup>37</sup>

The intermediacy of **II** in the alkoxide-dependent C–O reductive elimination pathway is supported by the presence of a facile, associative alkoxide-exchange pathway for **5**.<sup>37</sup> Likewise, both ligand-promoted C–C reductive elimination and ligand-promoted CO insertion have been observed. For example, reductive elimination from the nickel aryl methyl complexes (dmpe)Ni(Ar)Me [dmpe = (dimethylphosphino)et-

(34) Michelin, R. A.; Ros, R. *J. Organomet. Chem.* **1979**, *169*, C42.

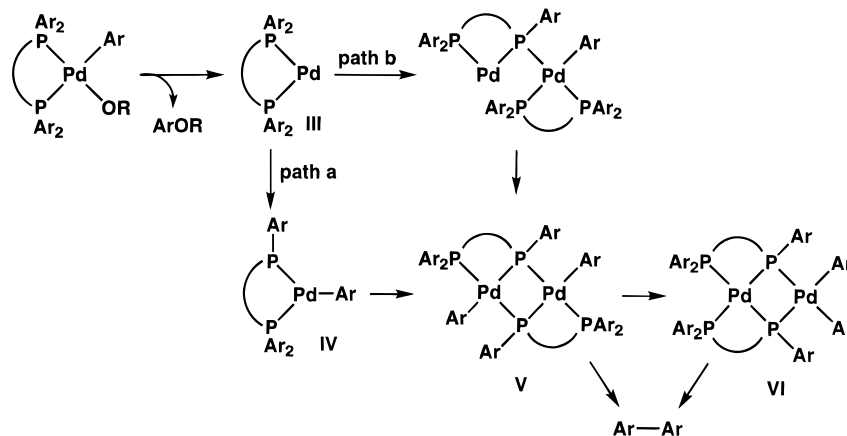
(35) (a) Kegley, S. E.; Schaverien, C. J.; Freudenberg, J. H.; Bergman, R. G.; Nolan, S. P.; Hoff, C. D. *J. Am. Chem. Soc.* **1987**, *109*, 6563. (b) Osakada, K.; Kim, Y.-J.; Yamamoto, A. *J. Organomet. Chem.* **1990**, *382*, 303. (c) Kim, Y. J.; Osakada, K.; Takenaka, A.; Yamamoto, A. *J. Am. Chem. Soc.* **1990**, *112*, 1096. (d) Osakada, K.; Kim, Y. J.; Tanaka, M.; Ishiguro, S.; Yamamoto, A. *Inorg. Chem.* **1991**, *30*, 197. (e) Shubina, E. S.; Belkova, N. V.; Krylov, A. N.; Vorontsov, E. V.; Epstein, L. M.; Gusev, D. G.; Niedermann, M.; Berke, H. *J. Am. Chem. Soc.* **1996**, *118*, 1105.

(36) Although data are limited, existing studies indicate that the rate of reductive elimination should increase with increasing steric interaction within the complex (a) Jones, W. D.; Kuykendall, V. L. *Inorg. Chem.* **1991**, *30*, 2615. (b) Brown, J. M.; Guiry, P. J. *Inorg. Chim. Acta* **1994**, *220*, 249.

(37) Thermolysis of [(*R*)-Tol-BINAP]Pd(*p*-C<sub>6</sub>H<sub>4</sub>NO<sub>2</sub>)(OCH<sub>2</sub>CMe<sub>3</sub>) [*σ*<sub>para</sub> NO<sub>2</sub> = 0.78] at 25 °C was ~100 times faster (ΔΔ*G*<sup>‡</sup> ≈ 3.5 kcal mol<sup>−1</sup>) than reductive elimination from **5** [*σ*<sub>para</sub> CN = 0.66], forming *p*-neopentoxynitrobenzene in >90% yield. Likewise, thermolysis of [dppf]Pd(*p*-C<sub>6</sub>H<sub>4</sub>-NO<sub>2</sub>)(OCH<sub>2</sub>CMe<sub>3</sub>) was considerably more facile than decomposition of **7**, occurring readily at 25 °C (*k*<sub>obs</sub> = 1.62 ± 0.2 s<sup>−1</sup>, ΔΔ*G*<sup>‡</sup> ≈ 2.3 kcal mol<sup>−1</sup>) with formation of *p*-neopentoxynitrobenzene in 81% yield. In contrast, extended thermolysis of either [(*S*)-BINAP]Pd(*p*-C<sub>6</sub>H<sub>4</sub>Cl)(OCH<sub>2</sub>CMe<sub>3</sub>) or (dppf)Pd(*p*-C<sub>6</sub>H<sub>4</sub>Cl)(OCH<sub>2</sub>CMe<sub>3</sub>) [*σ*<sub>para</sub> Cl = 0.23] led to slow decomposition with no detectable formation of *p*-neopentoxybenzonitrile: Widenhoefer, R. A.; Buchwald, S. L. Unpublished observations.

(38) Presumably, the Tol-BINAP ligand of **I** will span equatorial and axial sites in the trigonal bipyramid with a P–M–P bond angle ≈ 90°, close to the value of (~92°) observed in square planar palladium–BINAP complexes [Hayashi, T.; Konishi, M.; Kobori, Y.; Kumada, M.; Higuchi, T.; Hirotsu, K. *J. Am. Chem. Soc.* **1984**, *106*, 158]. Likewise, the palladium-bound aryl ligand is expected to occupy the second axial position in the trigonal bipyramid [Rossi, A. R.; Hoffmann, R. *Inorg. Chem.* **1975**, *14*, 365].

## Scheme 11



hane] was promoted by addition of tertiary phosphines such as  $\text{PEt}_3$ ,<sup>39,40</sup> while reductive elimination from the platinum bis-(phosphine)diaryl complex  $(\text{PPh}_3)_2\text{Pt}(p\text{-C}_6\text{H}_4\text{Me})_2$  was accelerated by addition of excess  $\text{PPh}_3$ .<sup>30</sup> In addition, migratory CO insertion into the methyl–molybdenum bond of the cyclopentadienyl tri(carbonyl) complex  $(\eta^5\text{-C}_5\text{H}_5)\text{Mo}(\text{CO})_3\text{CH}_3$  to form the acetyl molybdenum complex  $(\eta^5\text{-C}_5\text{H}_5)\text{Mo}(\text{CO})_2(\text{PMePh}_2)\text{-COCH}_3$  in the presence of  $\text{PMePh}_2$  in substituted tetrahydrofuran solvents occurred by competing first- and second-order pathways.<sup>41</sup>

**Biaryl Formation.** Thermolysis of palladium aryl alkoxide complexes, which forms aryl ethers, also led to the formation of varying amounts (12–27%) of biaryl side products. Exclusive formation of 4,4'-dimethylbiphenyl from thermolysis of **5** and exclusive formation of biphenyl from thermolysis of **6** implicates the phosphorus-bound aryl groups as the source of biaryl, while the formation of a statistical amount of 4-phenyltoluene from thermolysis of a mixture of **5** and **6** points to an intermolecular process for biaryl formation.<sup>19</sup> In addition, several observations indicate that P–C bond cleavage occurs subsequent to C–O reductive elimination. For example, no significant quantities of benzonitrile were incorporated into the biaryl side products. In addition, thermolysis of **5** in the presence of a trapping agent eliminated formation of 4,4'-dimethylbiphenyl but affected neither the rate of decomposition nor yield of aryl ether.

The above observations are in accord with biaryl formation via P–C oxidative addition<sup>18</sup> to the reactive<sup>28</sup> 14-electron fragment  $\text{Pd}[\text{P}-\text{P}]$  [ $\text{P}-\text{P} = \text{BINAP}, \text{Tol-BINAP}$ ] generated by C–O reductive elimination from a palladium (aryl)alkoxide complex (Scheme 10). In one possible mechanism, intramolecular P–C oxidative addition to  $\text{Pd}[\text{P}-\text{P}]$  followed by dimerization of the resulting mononuclear phosphido fragment **IV** would form the bridging phosphido dimer **V** (path a). Dinuclear reductive elimination<sup>42</sup> directly from **V** or ligand rearrangement followed by unimolecular reductive elimination from **VI** would then form biaryl. Alternatively,  $\mu$ -phosphido dimer **V** could also be generated via two consecutive intermolecular P–C oxidative additions to  $\text{Pd}[\text{P}-\text{P}]$  (path b). However, it appears somewhat unlikely that  $\text{Pd}[\text{P}-\text{P}]$  could attack a second

molecule of  $\text{Pd}[\text{P}-\text{P}]$  without also attacking the parent palladium aryl alkoxide complex prior to C–O reductive elimination, which was not observed. Phosphine degradation via P–C oxidative addition has also been observed in the thermal decomposition of the platinum diaryl bis(phosphine) complex  $(\text{PPh}_3)_2\text{Pt}(p\text{-C}_6\text{H}_4\text{Me})_2$ , which formed 4,4'-dimethylbiphenyl and biphenyl.<sup>43</sup>

## Conclusions

Thermal decomposition of palladium(aryl)alkoxide complexes led to C–O reductive elimination with formation of aryl ethers. Significantly, these transformations represent the first examples of C–O reductive elimination from group 10 metal (aryl)alkoxide complexes.<sup>8</sup> Thermolysis of these palladium aryl alkoxide complexes also formed biaryl side products derived from the palladium-bound aryl groups formed via intermolecular decomposition of the 14-electron  $\text{Pd}(0)$  fragment generated via initial reductive elimination. Kinetic analysis of the decomposition of  $[(R)\text{-Tol-BINAP}]\text{Pd}(p\text{-C}_6\text{H}_4\text{CN})(\text{OCH}_2\text{CMe}_3)$  (**5**) in the presence of excess alkoxide established a two-term rate law consistent with the presence of both an alkoxide-independent and alkoxide-dependent pathway for C–O reductive elimination. Significantly, unimolecular C–O reductive elimination appears to be initiated by inner-sphere nucleophilic attack of the alkoxide lone pair at the ipso carbon atom of the palladium-bound aryl group. Likewise, an alkoxide-dependent pathway initiated by direct attack of  $\text{KOCH}_2\text{CMe}_3$  at palladium was supported by the presence of an associative alkoxide-exchange pathway for **5**.

## Experimental Section

**General Methods.** All manipulations and reactions were performed under an atmosphere of nitrogen or argon in a glovebox or by standard Schlenk techniques. Preparative-scale reactions were performed in flame- or oven-dried Schlenk tubes equipped with a stir bar, side arm joint, and a septum. NMR spectra were obtained in oven-dried 5 mm thin-walled NMR tubes capped with a rubber septum on a Varian XL-300 spectrometer at 23 °C unless otherwise noted. Gas chromatography was performed on a Hewlett-Packard Model 5890 gas chromatograph using a 25 m polymethylsiloxane capillary column. Elemental analyses were performed by E+R Microanalytical Laboratories (Corona, NY). Diethyl ether, hexane, and  $\text{THF-d}_8$  were distilled from solutions of sodium/benzophenone ketyl under argon or nitrogen.  $\text{Pd}_2(\text{DBA})_3$ ,  $\text{P}(o\text{-tol})_3$ ,  $(R)\text{-Tol-BINAP}$ ,  $(S)\text{-Tol-BINAP}$ ,  $\text{dppf}$  (Strem),  $(S)\text{-BINAP}$  (Pfizer), 4-bromobenzonitrile, 4-iodobenzonitrile, pivaldehyde, biphenyl, 4,4'-dimethylbiphenyl,  $p$ -phenylbenzonitrile, 4-phenyltoluene, and benzonitrile (Aldrich) were used as received. KOTf and KBr (Aldrich)

(39) Komiya, S.; Abe, Y.; Yamamoto, A.; Yamamoto, T. *Organometallics* **1983**, *2*, 1466.

(40) Tatsumi, K.; Nakamura, A.; Komiya, S.; Yamamoto, A.; Yamamoto, T. *J. Am. Chem. Soc.* **1984**, *106*, 8181.

(41) Wax, M. J.; Bergman, R. G. *J. Am. Chem. Soc.* **1981**, *103*, 7028.

(42) (a) Hersh, W. H.; Bergman, R. G. *J. Am. Chem. Soc.* **1983**, *105*, 5846. (b) Hembre, R. T.; Scott, C. P.; Norton, J. R. *J. Org. Chem.* **1987**, *52*, 3650. (c) Chetcuti, M. J.; Chisholm, M. H.; Folting, K.; Haitko, D. A.; Huffman, J. C. *J. Am. Chem. Soc.* **1982**, *104*, 2138. (d) Halpern, J. *Inorg. Chim. Acta* **1982**, *62*, 31.

(43) Braterman, P. S.; Cross, R. J.; Young, G. B. *J. Chem. Soc., Chem. Commun.* **1976**, 1310.

were dried under vacuum at 220 °C prior to use. Potassium alkoxides were synthesized from reaction of anhydrous alcohol with 1 equiv of KH in THF.

**{Pd[P(*o*-tolyl)<sub>3</sub>](*p*-C<sub>4</sub>H<sub>4</sub>CN)(*μ*-Br)}<sub>2</sub>.** A purple solution of Pd<sub>2</sub>(DBA)<sub>3</sub> (1.0 g, 1.1 mmol), P(*o*-tol)<sub>3</sub> (1.3 g, 4.3 mmol), and *p*-bromobenzonitrile (2.0 g, 11 mmol) in benzene (60 mL) was stirred at room temperature for 1 h. The resulting green/brown solution was filtered through Celite, and benzene was evaporated under vacuum. The oily residue was dissolved in Et<sub>2</sub>O (25 mL) and allowed to stand at room temperature overnight. The resulting yellow precipitate was filtered, washed with Et<sub>2</sub>O, and dried under vacuum to give {Pd[P(*o*-tolyl)<sub>3</sub>](*p*-C<sub>4</sub>H<sub>4</sub>CN)(*μ*-Br)}<sub>2</sub> (0.95 g, 75%) as a yellow powder. <sup>1</sup>H NMR (CHCl<sub>3</sub>, 55 °C): δ 7.33, 7.13, 6.90, 6.73, 2.10. <sup>31</sup>P{<sup>1</sup>H} NMR (CDCl<sub>3</sub>, 55 °C): δ ~22.5 (br s). IR (THF): ν<sub>(C=N)}</sub> 2222 cm<sup>-1</sup>. Anal. Calcd for C<sub>56</sub>H<sub>50</sub>Br<sub>2</sub>N<sub>2</sub>P<sub>2</sub>D<sub>2</sub> (found): C, 56.73 (56.57); H, 4.25 (4.51).

**{Pd[P(*o*-tolyl)<sub>3</sub>](*p*-C<sub>6</sub>H<sub>4</sub>CN)(*μ*-I)}<sub>2</sub>.** Reaction of Pd<sub>2</sub>(DBA)<sub>3</sub> (1.0 g, 1.1 mmol), P(*o*-tol)<sub>3</sub> (1.3 g, 4.3 mmol), and *p*-iodobenzonitrile (1.75 g, 8.6 mmol) in benzene (60 mL) employing a procedure analogous to that used to synthesize {Pd[P(*o*-tolyl)<sub>3</sub>](*p*-C<sub>4</sub>H<sub>4</sub>CN)(*μ*-Br)}<sub>2</sub> led to the isolation of {Pd[P(*o*-tolyl)<sub>3</sub>](*p*-C<sub>6</sub>H<sub>4</sub>CN)(*μ*-I)}<sub>2</sub> (1.17 g, 84%) as a yellow powder. Anal. Calcd for C<sub>56</sub>H<sub>50</sub>I<sub>2</sub>N<sub>2</sub>P<sub>2</sub>D<sub>2</sub> (found): C, 52.57 (52.80); H, 3.94 (4.12).

**[(*R*)-Tol-BINAP]Pd(*p*-C<sub>4</sub>H<sub>4</sub>CN)(Br) (1).** A solution of {Pd[P(*o*-tolyl)<sub>3</sub>](*p*-C<sub>4</sub>H<sub>4</sub>CN)(*μ*-Br)}<sub>2</sub> (200 mg, 0.17 mmol) and (*R*)-Tol-BINAP (240 mg, 0.35 mmol) in CH<sub>2</sub>Cl<sub>2</sub> (10 mL) was stirred at room temperature for 5 h and then evaporated under vacuum. The oily residue was dissolved in Et<sub>2</sub>O (10 mL) and allowed to stand at room temperature for 4 h. The resulting precipitate was filtered, washed with Et<sub>2</sub>O, and dried under vacuum to give **1** (308 mg, 94%) as a cream-colored solid that contained traces of ether (<5%) by <sup>1</sup>H NMR analysis. <sup>1</sup>H NMR (THF-*d*<sub>8</sub>): δ 8.26 (dd, *J* = 8.7, 10.5 Hz), 8.04 (t, *J* = 8.2 Hz), 7.98 (t, *J* = 9.3 Hz), 7.91 (q, *J* = 7.7 Hz), 7.77–7.60 (m, 7 H), 7.38 (m, 4 H), 7.28–7.14 (m, 5 H), 6.90 (d, *J* = 8.4 Hz, 1 H), 6.77 (d, *J* = 6.8 Hz, 2 H), 6.67 (d, *J* = 7.0 Hz, 2 H), 2.76 (s, 3 H), 2.56 (s, 3 H), 2.31 (s, 3 H), 2.29 (s, 3 H). <sup>31</sup>P{<sup>1</sup>H}NMR: δ 26.7 (d, *J* = 38.1 Hz), 11.4 (d, *J* = 37.9 Hz). IR (THF): ν<sub>(C=N)}</sub> 2219 cm<sup>-1</sup>. Anal. Calcd for C<sub>55</sub>H<sub>44</sub>BrNP<sub>2</sub>D (found): C, 68.30 (68.36); H, 4.59 (4.87).

**[(*S*)-Tol-BINAP]Pd(*p*-C<sub>6</sub>H<sub>4</sub>CN)(I) (2).** Reaction of {Pd[P(*o*-tolyl)<sub>3</sub>](*p*-C<sub>4</sub>H<sub>4</sub>CN)(*μ*-I)}<sub>2</sub> (230 mg, 0.36 mmol) and (*S*)-Tol-BINAP (250 mg, 0.37 mmol) employing a procedure analogous to that used to synthesize **1** led to the isolation of **2** (273 mg, 75%) as a yellow powder. <sup>1</sup>H NMR (THF-*d*<sub>8</sub>): δ 7.99 (dd, *J* = 10.2, 10.5 Hz, 1 H), 7.83 (dd, *J* = 8.7, 1.5 Hz, 1 H), 7.70–7.55 (m, 6 H), 7.50–6.80 (m, 19 H), 6.53 (d, *J* = 8.7 Hz, 1 H), 6.44 (d, *J* = 6.9 Hz, 2 H), 6.32 (d, *J* = 6.9 Hz, 2 H), 2.42 (s, 3 H), 2.20 (s, 3 H), 1.96 (s, 3 H), 1.95 (s, 3 H). <sup>31</sup>P{<sup>1</sup>H}NMR: δ 20.4 (d, *J* = 38.6 Hz), 8.9 (d, *J* = 38.6 Hz). Anal. Calcd for C<sub>55</sub>H<sub>44</sub>INP<sub>2</sub>D (found): C, 65.13 (65.17); H, 4.37 (4.64).

**[(*S*)-BINAP]Pd(*p*-C<sub>6</sub>H<sub>4</sub>CN)(Br) (3).** Reaction of {Pd[P(*o*-tolyl)<sub>3</sub>](*p*-C<sub>4</sub>H<sub>4</sub>CN)(*μ*-Br)}<sub>2</sub> (200 mg, 0.17 mmol) and (*S*)-BINAP (220 mg, 0.35 mmol) using a procedure analogous to that used to form **1** gave **3** (246 mg, 80%) as a white solid that contained traces of ether (<5%) by <sup>1</sup>H NMR analysis. <sup>1</sup>H NMR (THF-*d*<sub>8</sub>): δ 8.01 (t, *J* = 8.8 Hz, 1 H), 7.81 (d, *J* = 9.3 Hz, 3 H), 7.68–7.54 (m, 6 H), 7.46 (s, 6 H), 7.39 (t, *J* = 7.8 Hz, 1 H), 7.33 (t, *J* = 7.3 Hz, 1 H), 7.20–7.06 (m, 5 H), 7.04–6.94 (m, 6 H), 6.80–6.50 (m, 7 H). <sup>31</sup>P{<sup>1</sup>H}NMR: δ 27.9 (d, *J* = 38.4 Hz), 12.9 (d, *J* = 38.4 Hz). Anal. Calcd for C<sub>51</sub>H<sub>36</sub>BrNP<sub>2</sub>D (found): C, 67.23 (67.02); H, 3.98 (4.20).

**(dppf)Pd(*p*-C<sub>4</sub>H<sub>4</sub>CN)(Br) (4).** A solution of {Pd[P(*o*-tolyl)<sub>3</sub>](*p*-C<sub>4</sub>H<sub>4</sub>CN)(*μ*-Br)}<sub>2</sub> (200 mg, 0.17 mmol) and dppf (258 mg, 0.47 mmol) in CH<sub>2</sub>Cl<sub>2</sub> (10 mL) was stirred at room temperature for 12 h. The resulting solution was concentrated under vacuum. Addition of Et<sub>2</sub>O (10 mL) formed a precipitate that was filtered, washed with Et<sub>2</sub>O, and dried under vacuum to give **4** (280 mg, 79%) as a bright yellow solid that contained traces of ether (<5%) by <sup>1</sup>H NMR analysis. <sup>1</sup>H NMR (CDCl<sub>3</sub>): δ 8.01 (dt, *J* = 2.7, 9.7 Hz), 7.47 (m, 6 H), 7.33 (t, *J* = 11.2 Hz, 6 H), 7.12 (dt, *J* = 1.7, 15.4 Hz, 6 H), 6.76 (d, *J* = 7.54 Hz, 2 H), 4.68 (d, *J* = 1.95 Hz, 2 H), 4.51 (s, 2 H), 4.14 (d, *J* = 2.23 Hz, 2 H), 3.59 (d, *J* = 1.74 Hz, 2 H). <sup>31</sup>P{<sup>1</sup>H}NMR (CDCl<sub>3</sub>): δ 30.0 (d, *J* = 29.2 Hz), 10.8 (d, *J* = 31.6 Hz). IR (CH<sub>2</sub>Cl<sub>2</sub>): ν<sub>(C=N)}</sub> 2220 cm<sup>-1</sup>. Anal. Calcd for C<sub>41</sub>H<sub>32</sub>BrFeNP<sub>2</sub>D (found): C, 58.43 (58.41); H, 3.83 (3.98).

**[(*R*)-Tol-BINAP]Pd(*p*-C<sub>6</sub>H<sub>4</sub>CN)(OCH<sub>2</sub>CMe<sub>3</sub>) (5).** A 0.54 M solution of KOCH<sub>2</sub>Me<sub>3</sub> in THF-*d*<sub>8</sub> (25 μL, 1.35 × 10<sup>-2</sup> mmol) was added

via syringe to a colorless solution of **1** (12 mg, 1.25 × 10<sup>-2</sup> mmol) and PhSiMe<sub>3</sub> (1.75 mg, 1.16 × 10<sup>-2</sup> mmol) in THF-*d*<sub>8</sub> (0.70 mL). The tube was shaken briefly at room temperature to form an orange solution of **5** in quantitative (98 ± 5%) yield by <sup>1</sup>H NMR spectroscopy versus PhSiMe<sub>3</sub> internal standard, along with a small resonance corresponding to free alkoxide (δ 0.85). **5** was thermally unstable and was analyzed without isolation by <sup>1</sup>H and <sup>31</sup>P NMR spectroscopy. <sup>1</sup>H NMR (THF-*d*<sub>8</sub>): δ 7.83 (t, *J* = 8.4 Hz), 7.78–7.59 (m), 7.51–7.25 (m), 7.12 (t, *J* = 7.4 Hz), 7.04–6.93 (m), 6.81 (d, *J* = 7.0 Hz), 6.44 (d, *J* = 7.4 Hz), 6.29 (d, *J* = 7.4 Hz) 2.76 (d, *J* = 9.0 Hz, 1 H), 2.62 (d, *J* = 8.8 Hz, 1 H), 2.38 (s, 3 H), 2.19 (s, 3 H), 1.98 (s, 3 H), 1.93 (s, 3 H), 0.17 (s, 9 H). <sup>31</sup>P{<sup>1</sup>H}NMR (THF-*d*<sub>8</sub>): δ 29.3 (d, *J* = 36.6 Hz), 14.1 (d, *J* = 36.7 Hz). IR (THF): ν<sub>(C=N)}</sub> 2218 cm<sup>-1</sup>.

**[(*S*)-BINAP]Pd(*p*-C<sub>6</sub>H<sub>4</sub>CN)(OCH<sub>2</sub>CMe<sub>3</sub>) (6).** Reaction of KOCH<sub>2</sub>Me<sub>3</sub> (1.6 mg, 1.25 × 10<sup>-2</sup> mmol) and **3** (11 mg, 1.21 × 10<sup>-2</sup> mmol) using a procedure analogous to that used to form **5** generated a bright yellow solution of **6**. <sup>1</sup>H NMR (THF-*d*<sub>8</sub>): δ 7.90 (m), 7.69 (m), 7.61 (t, *J* = 9.0 Hz), 7.44 (m), 7.14 (d, *J* = 8.5 Hz), 6.99 (t, *J* = 9.3 Hz), 6.69 (t, *J* = 7.3 Hz), 6.52 (br s), 2.79 (d, *J* = 8.5 Hz, 1 H), 2.62 (d, *J* = 8.5 Hz, 1 H), 0.16 (s, 9 H). <sup>31</sup>P{<sup>1</sup>H} NMR (THF-*d*<sub>8</sub>): δ 31.7 (d, *J* = 37.2 Hz), 15.5 (d, *J* = 37.1 Hz).

**[(*R*)-Tol-BINAP]Pd(*p*-C<sub>6</sub>H<sub>4</sub>CN)(OCHMe<sub>2</sub>) (7).** Reaction of KOCHMe<sub>2</sub> and **1** using a procedure analogous to that used to prepare **5** gave **7** in ~90% yield along with minor decomposition products and a small resonance corresponding to free alkoxide. **7** was thermally unstable and was analyzed without isolation by <sup>1</sup>H and <sup>31</sup>P NMR spectroscopy at -15 °C. <sup>1</sup>H NMR (THF-*d*<sub>8</sub>, -15 °C): δ 8.16 (t, *J* = 8.81 Hz, 2 H), 7.63 (m, 4 H), 7.55 (d, *J* = 7.26 Hz, 2 H), 7.44 (d, *J* = 10.1 Hz, 2 H), 7.36 (m, 4 H), 7.20 (d, *J* = 7.31 Hz, 2 H), 7.10 (m, 4 H), 6.93 (d, *J* = 7.46 Hz, 2 H), 6.87 (d, *J* = 7.20, 2 H), 6.77 (d, *J* = 8.32 Hz, 2 H), 6.66 (d, *J* = 8.39 Hz, 2 H), 6.37 (br s, 4 H), 3.21 (m, 1 H), 2.36 (s, 3 H), 2.25 (s, 3 H), 1.95 (s, 3 H), 1.94 (s, 3 H), 0.65 (d, *J* = 5.8 Hz, 3 H), 0.63 (d, *J* = 5.8 Hz, 3 H). <sup>31</sup>P{<sup>1</sup>H}NMR (THF-*d*<sub>8</sub>, -15 °C): δ 30.2 (d, *J* = 36.7 Hz), 14.2 (d, *J* = 37.4 Hz).

**[(*R*)-Tol-BINAP]Pd(*p*-C<sub>6</sub>H<sub>4</sub>CN)(OCMe<sub>3</sub>) (8).** Reaction of **1** (12 mg, 1.2 × 10<sup>-2</sup> mmol) and KOCMe<sub>3</sub> (0.95 mg, 0.013 mmol) employing a procedure analogous to that used to generate **5** gave **8** in 82 ± 5% yield by <sup>1</sup>H NMR analysis. **8** was thermally unstable and was analyzed without isolation by <sup>1</sup>H and <sup>31</sup>P NMR spectroscopy. <sup>1</sup>H NMR (22 °C, THF-*d*<sub>8</sub>): in addition to a small resonance corresponding to free alkoxide (δ 1.15), resonances were observed at δ 7.94 (t, *J* = 8.1 Hz), 7.68 (q, *J* = 9.3 Hz), 7.60 (d, *J* = 8.6 Hz), 7.46 (t, *J* = 7.1 Hz, 2 H), 7.35 (q, *J* = 8.3 Hz), 7.23 (d, *J* = 7.9 Hz), 7.13 (t, *J* = 8.1 Hz), 7.00 (t, *J* = 7.9 Hz), 6.86 (dd, *J* = 2.0, 8.2 Hz), 6.68 (t, *J* = 9.4 Hz, 2 H), 6.38 (d, 2 H, *J* = 7.3 Hz), 6.31 (d, *J* = 7.0 Hz, 2 H), 2.38 (s, 3 H), 2.28 (s, 3 H), 1.97 (s, 3 H), 1.90 (s, 3 H), 0.54 (s, 9 H). <sup>31</sup>P{<sup>1</sup>H}NMR (22 °C, THF-*d*<sub>8</sub>): δ 25.2 (d, *J* = 40.0 Hz), 12.1 (d, *J* = 39.8 Hz). IR (THF): ν<sub>(C=N)}</sub> 2218 cm<sup>-1</sup>.

**[(*R*)-Tol-BINAP]Pd(*p*-C<sub>6</sub>H<sub>4</sub>CN)(OC<sub>6</sub>H<sub>4</sub>Me) (9).** A solution of potassium *p*-cresolate (26 mg, 0.18 mmol) and **2** (180 mg, 0.18 mmol) in THF (15 mL) was stirred at room temperature for 15 min, and the resulting orange solution was filtered through Celite. Concentration of solvent under vacuum (~3 mL) and dropwise addition of hexane (20 mL) formed a precipitate that was washed with ether and dried under vacuum to give **9** (164 mg, 89%) as orange microcrystals. <sup>1</sup>H NMR (C<sub>6</sub>D<sub>6</sub>): δ 7.96 (dd, *J* = 8.4, 10.6 Hz), 7.84 (t, *J* = 8.9 Hz), 7.67 (t, *J* = 8.6 Hz), 7.61 (m), 7.31 (dd, *J* = 8.13, 11.3 Hz), 7.28 (t, *J* = 10.0 Hz), 7.18 (t, *J* = 8.73 Hz), 6.96 (m), 6.85 (q, *J* = 8.9 Hz), 6.70 (dd, *J* = 2.1, 8.14 Hz), 6.57 (m), 6.24 (d, *J* = 7.05 Hz), 6.14 (d, *J* = 7.05 Hz), 2.19 (s, 3 H), 1.98 (s, 3 H), 1.87 (s, 3 H), 1.71 (s, 6 H). <sup>31</sup>P{<sup>1</sup>H}NMR (C<sub>6</sub>D<sub>6</sub>): δ 31.1 (d, *J* = 38.3 Hz), 14.4 (d, *J* = 38.3 Hz). Although solutions of **9** were homogeneous and >95% pure by <sup>1</sup>H and <sup>31</sup>P NMR analysis, C analysis was consistently low and H analysis was consistently high. Anal. Calcd for C<sub>62</sub>H<sub>51</sub>NOP<sub>2</sub>D (found): C, 74.88 (73.13); H, 5.17 (5.74). Reaction of KOC<sub>6</sub>H<sub>4</sub>Me with bromide precursor **1** provided **9** which was spectroscopically and analytically identical to that generated from **2**.

**(dppf)Pd(*p*-C<sub>6</sub>H<sub>4</sub>CN)(OCH<sub>2</sub>CMe<sub>3</sub>) (10).** A yellow suspension of **4** (11 mg, 1.3 × 10<sup>-2</sup> mmol) in THF-*d*<sub>8</sub> (0.70 mL) was treated with aliquots of KOCH<sub>2</sub>Me<sub>3</sub> in THF-*d*<sub>8</sub>. Addition of 1.1 equiv of alkoxide formed an orange solution of **10** and a small amount of free KOCH<sub>2</sub>Me<sub>3</sub> as the exclusive products by <sup>1</sup>H NMR spectroscopy. Despite the



relatively slow decomposition of **10** at room temperature ( $t_{1/2} \approx 4$  h), attempts to isolate **10** from the corresponding preparative-scale reaction gave only impure brown solids.  $^1\text{H}$  NMR (22 °C, THF- $d_8$ ):  $\delta$  8.21 (m, 4 H), 7.46 (m), 7.40 (d,  $J = 11.5$  Hz), 7.37 (dd,  $J = 1.2, 11.6$  Hz), 7.31 (t,  $J = 7.3$  Hz), 7.09 (dt,  $J = 2.1, 8.0$  Hz), 6.75 (dd,  $J = 2.2, 8.2$  Hz, 2 H), 4.82 (q,  $J = 2.0$  Hz, 2 H), 4.58 (br s, 2 H), 4.20 (t,  $J = 1.6$  Hz, 2 H), 3.55 (q,  $J = 1.8$  Hz, 2 H), 2.68 (s, 2 H), 0.23 (s, 9 H).  $^{31}\text{P}\{^1\text{H}\}$ NMR (22 °C, THF- $d_8$ ):  $\delta$  30.9 (d,  $J = 32$  Hz), 11.9 (d,  $J = 31.7$  Hz). IR (THF):  $\nu_{\text{C=N}}$  2218  $\text{cm}^{-1}$ .

**(dppf)Pd(*p*-C<sub>6</sub>H<sub>4</sub>CN)(OCMe<sub>3</sub>) (11).** Reaction of **4** (11 mg,  $1.3 \times 10^{-2}$  mmol) and KOCH<sub>2</sub>CMe<sub>3</sub> (1.05 mg,  $1.4 \times 10^{-2}$  mmol) employing a procedure analogous to that used to generate **10** gave **11** as the exclusive product by  $^1\text{H}$  NMR analysis. **11** was thermally unstable and was analyzed without isolation by  $^1\text{H}$  and  $^{31}\text{P}$  NMR spectroscopy.  $^1\text{H}$  NMR (22 °C, THF- $d_8$ ):  $\delta$  8.25 (br t,  $J = 8.4$  Hz, 4 H), 7.46 (m), 7.39 (d,  $J = 7.5$  Hz), 7.35 (d,  $J = 8.0$  Hz), 7.29 (d,  $J = 8.1$  Hz), 7.25 (s), 7.08 (br t,  $J = 7.5$  Hz, 4 H), 6.67 (br d,  $J = 7.8$  Hz, 2 H), 4.84 (br d,  $J = 1.86$  Hz, 2 H), 4.59 (br s, 2 H), 4.15 (br s, 2 H), 3.48 (br d,  $J = 1.68$  Hz, 2 H), 0.46 (s, 9 H).  $^{31}\text{P}\{^1\text{H}\}$ NMR (22 °C, THF- $d_8$ ):  $\delta$  33.1 (d,  $J = 36.8$  Hz), 11.7 (d,  $J = 36.7$  Hz). IR (THF):  $\nu_{\text{C=N}}$  2219  $\text{cm}^{-1}$ .

**(dppf)Pd[*o*-C<sub>6</sub>H<sub>4</sub>CH<sub>2</sub>CH<sub>2</sub>C(Me)<sub>2</sub>O] (12).** A suspension of Pd(dppf)[*o*-C<sub>6</sub>H<sub>4</sub>CH<sub>2</sub>CH<sub>2</sub>C(Me)<sub>2</sub>OH](Br) (50 mg, 0.55 mmol) and dry KH (15 mg, 0.38 mmol) in THF (3 mL) was stirred at room temperature for 3 min. The resulting yellow solution was filtered through Celite into hexane (10 mL), and the filtrate was concentrated under vacuum to 2.5 mL. The resulting precipitate was collected, washed with pentane, and dried under vacuum to give **12** (35 mg, 77% yield) as a yellow powder.  $^1\text{H}$  NMR: 8.39 (t,  $J = 8.1$  Hz, 2 H), 8.18 (t,  $J = 8.4$  Hz, 2 H), 7.61 (dd,  $J = 7.7, 11$  Hz, 2 H), 7.45 (m, 2 H), 7.30 (m, 8 H), 7.12 (q,  $J = 8.0$  Hz, 2 H), 6.96 (t,  $J = 6.38$  Hz, 2 H), 6.58 (dt,  $J = 3.4, 12.0$  Hz, 1 H), 6.50 (br d,  $J = 4.8$  Hz), 6.42 (t,  $J = 7.2$  Hz, 1 H), 6.17 (t,  $J = 7.1$  Hz), 4.83 (br s, 2 H), 4.55 (s, 1 H), 4.52 (s, 1 H), 4.17 (br s, 2 H), 4.08 (dt,  $J = 6.3, 12.7$  Hz, 1 H), 3.71 (s, 1 H), 3.43 (s, 1 H), 2.58 (dd, 3.8, 11.5, 1 H), 1.75 (m, 1 H, partially obscured by THF), 1.52 (dt, 5.7, 12.8, 1 H), 0.55 (s, 3 H), 0.07 (s, 3 H).  $^{31}\text{P}\{^1\text{H}\}$ NMR (THF- $d_8$ ):  $\delta$  35.0 (d,  $J = 38.4$  Hz), 11.6 (d,  $J = 38.4$  Hz). Anal. Calcd for C<sub>15</sub>H<sub>12</sub>FeO<sub>2</sub>Pd (found): C, 65.67 (65.51); H, 5.14 (5.33).

**Kinetic Measurements.** Samples for kinetic analysis were prepared from stock solutions of the appropriate palladium aryl halide complex and were performed in oven-dried 5 mm thin-walled NMR tubes capped with rubber septa. Solvent volume in the NMR tubes was calculated from the solvent height measured at 25 °C according to the relationship  $V$  (mL) =  $H$  (mm)  $\times$  0.01384 – 0.006754 and from the temperature dependence of the density of benzene.<sup>44</sup> Kinetic data were obtained by  $^1\text{H}$  NMR spectroscopy in the heated probe of a Varian XL-300 spectrometer. Probe temperatures were measured with an ethylene glycol thermometer and were maintained at  $\pm 0.5$  °C throughout data acquisition. Syringes employed in measuring liquids for kinetic measurements were calibrated by mercury displacement and were accurate to >95%. Error limits for rate constants refer to the standard deviation of the corresponding least-squares-fit line or to the standard deviation of two or more separate experiments.

**Thermolysis of 5.** An NMR tube containing a freshly prepared solution of **5** (12 mg,  $1.2 \times 10^{-2}$  mmol) and PhSiMe<sub>3</sub> (1.75 mg,  $1.16 \times 10^{-2}$  mmol) in THF- $d_8$  (0.70 mL) ([KOCH<sub>2</sub>CMe<sub>3</sub>]  $\approx$  1.7 mM) was placed in the probe of an NMR spectrometer heated at 47 °C. The concentrations of **5** and *p*-neopentoxybenzotrile were determined by integrating the *tert*-butyl resonances for **5** ( $\delta$  0.17) and *p*-neopentoxybenzotrile ( $\delta$  1.06) versus the trimethylsilyl resonance of PhSiMe<sub>3</sub> ( $\delta$  0.25) in the  $^1\text{H}$  NMR spectrum. The concentrations of 4,4'-dimethylbiphenyl and benzotrile were determined by integration of

the respective peaks in the GC spectrum versus the integration of PhSiMe<sub>3</sub>. The first-order rate constant for disappearance of **5** was determined from a plot of  $\ln \{[\mathbf{5}]_t/[\mathbf{5}]_0\}$  versus time (Table 1). The corresponding plot of reciprocal concentration versus time deviated considerably from linearity. Kinetics and product analysis for thermolysis of complexes **6–9** were performed analogously.

First-order rate constants for disappearance of **5** in the absence of added KOCH<sub>2</sub>CMe<sub>3</sub> (<2 mM) were also obtained at 23, 35, 37, 52, and 57 °C (Table 1); activation parameters were obtained from a plot  $\ln \{k/T\}$  versus  $1/T$  (Figure 2). First-order rate constants for disappearance of **5** were also measured as a function of [KOCH<sub>2</sub>CMe<sub>3</sub>] from 0.043 to 0.30 M at 47 °C in THF- $d_8$  (Table 1). Solutions of **5** with KOCH<sub>2</sub>CMe<sub>3</sub> concentrations ranging from 0.43 to 0.12 M were obtained by a procedure analogous to that described above. Solutions of **5** with KOCH<sub>2</sub>CMe<sub>3</sub> concentrations >0.12 M were prepared by adding a THF- $d_8$  solution of **5** (17 mM) via syringe to an NMR tube containing solid KOCH<sub>2</sub>CMe<sub>3</sub>. The first-order rate constant  $k$  was obtained as the intercept of a plot of  $k_{\text{obs}}$  versus [KOCH<sub>2</sub>CMe<sub>3</sub>] (Figure 3). The second-order rate constant  $k'$  was obtained from the slope of this plot.

**Alkoxide Exchange with 5.** An NMR tube containing a freshly prepared solution of **5** (12 mg,  $1.2 \times 10^{-2}$  mmol, 19 mM), PhSiMe<sub>3</sub> (1.75 mg,  $1.16 \times 10^{-2}$  mmol), and KOCH<sub>2</sub>CMe<sub>3</sub> (3.4 mg, 0.0271 mmol, 0.043 mM) in THF- $d_8$  (0.63 mL) was placed in the probe of an NMR spectrometer heated at 47 °C. The excess line broadening ( $\Delta\omega_{1/2}$ ) of the *tert*-butyl resonance of **5** was determined by measuring the peak width at half-height ( $\omega_{1/2}$ ) for the *tert*-butyl resonance of **5** ( $\delta$  0.17) relative to  $\omega_{1/2}$  for the trimethylsilyl resonance of PhSiMe<sub>3</sub> ( $\delta$  0.25) in the  $^1\text{H}$  NMR spectrum [ $\Delta\omega_{1/2}(\mathbf{5}) = \omega_{1/2}(\mathbf{5}) - \omega_{1/2}(\text{PhTMS})$ ]. Because the separation of the *tert*-butyl peaks for PdOCH<sub>2</sub>CMe<sub>3</sub> and KOCH<sub>2</sub>CMe<sub>3</sub> ( $\Delta\nu > 200$  Hz) was much larger than the excess broadening of the *tert*-butyl resonance of **5** ( $\omega_{1/2} = 5.5$  Hz), the slow-exchange approximation ( $\Delta\omega_{1/2} = k_{\text{obs}}/\pi$ ) was employed to convert  $\Delta\omega_{1/2}$  to  $k_{\text{obs}}$ .<sup>17</sup> Observed rate constants for alkoxide exchange were also determined at KOCH<sub>2</sub>CMe<sub>3</sub> concentrations ranging from 0.0017 to 0.30 M. The second-order rate constant  $k_{\text{ex}}$  for exchange of alkoxide with **5** was determined from the slope of a plot of  $k_{\text{obs}}$  versus [KOCH<sub>2</sub>CMe<sub>3</sub>] (Figure 4).

**Thermolysis of 10.** An NMR tube containing a freshly prepared solution of **10** (11 mg,  $1.2 \times 10^{-2}$  mmol, 18 mM) and mesitylene (1.72 mg,  $1.14 \times 10^{-2}$  mmol) in THF- $d_8$  (0.70 mL) was placed in the probe of an NMR spectrometer preheated to 55 °C. The concentrations of **10**, *p*-neopentoxybenzotrile, and pivaldehyde were determined by integrating the *tert*-butyl resonances for **7** ( $\delta$  0.23), *p*-neopentoxybenzotrile ( $\delta$  1.06), and pivaldehyde ( $\delta$  1.04) versus the methyl resonance of mesitylene ( $\delta$  2.12) in the  $^1\text{H}$  NMR spectrum. The concentrations of biphenyl and benzotrile were determined from the integration of the respective peaks in the GC spectrum versus the mesitylene peak. The first-order rate constant for disappearance of **10** was determined from a plot of  $\ln \{[\mathbf{10}]_t/[\mathbf{10}]_0\}$  versus time (Table 1). Kinetics and product analysis for thermolysis of complexes **11** and **12** were performed analogously.

**Acknowledgment.** We thank the National Science Foundation, Dow Chemical, and Pfizer for their support of this work. R.W. is an NCI Postdoctoral Trainee supported by NIH Cancer Training Grant No. CI T32CA09112. We thank Dr. M. Palucki for providing samples of *p*-neopentoxybenzotrile, *p*-isopropoxybenzotrile, and *p*-*tert*-butoxybenzotrile, and we thank Mr. J. P. Wolfe for providing a sample of (dppf)Pd[*o*-C<sub>6</sub>H<sub>4</sub>(CH<sub>2</sub>)<sub>2</sub>C(Me)<sub>2</sub>OH]Br. We would like to thank a reviewer for several insightful suggestions including the possibility of an alkoxide-promoted reductive elimination pathway.

JA963324P

(44) *International Critical Tables of Numerical Data, Physics, Chemistry, and Technology*; Washburn, E. W., Ed.; McGraw-Hill: London, 1928; Vol. III, pp 29, 39, 221.